JOURNAL OF CATALYSIS 132, 183–199 (1991)

Catalytic Cooperation between MoO_3 and Sb_2O_4 in N-Ethyl Formamide Dehydration

II. Nature of Active Sites and Role of Spillover Oxygen

BING ZHOU,[1] TADEUSZ MACHEJ,[2] PATRICIO RUIZ, AND BERNARD DELMON

Catalyse et Chimie des Matériaux Divisés, Université Catholique de Louvain, Place Croix du Sud 1, 1348 Louvain-la-Neuve, Belgium

Received January 19, 1990; revised March 27, 1991

The present work reports experiments designed to further investigate the role of MoO_3 and Sb_2O_4 in the cooperative effect they exhibit in N-ethyl formamide dehydration. Temperature-programmed desorption of NH_3 showed that Brønsted acid sites are responsible for activity. TPD of CO_2 gave no indication of basic sites. The Brønsted sites are sensitive to reduction and reoxidation. Thermoreoxidation of previously reduced molybdenum oxide and oxidation of carbon deposited on MoO_3 are more rapid when α-Sb_2O_4 is admixed. The interpretation of the phenomenon is that α-Sb_2O_4 dissociates molecular O_2 to an oxygen spillover species which can maintain MoO_3 at a high degree of oxidation and, if necessary, reoxidize it or remove deposited carbon. Brønsted sites necessitate a high degree of oxidation and their number is consequently promoted by spillover oxygen. Mechanisms are proposed for the dissociation of oxygen, the reoxidation of pre-reduced MoO_3, and the formation of Brønsted acid sites. The importance of the reported results for selective oxidation or multicomponent catalysts is discussed.

1. INTRODUCTION

In the preceding paper of this series (*1*), the catalytic synergy in the dehydration of N-ethyl formamide to propionitrile was explained by a remote control mechanism according to which active sites situated on MoO_3 (controlled phase or acceptor A) would be created or regenerated by the action of a mobile species (spillover oxygen) formed on α-Sb_2O_4 (controlling phase or donor D). To give further support to the proposed mechanism, it is essential to investigate the nature of the active sites and to analyse, in greater detail, the role of spillover oxygen.

For this purpose, we must first of all summarize the reports in the literature concerning acidity in catalysts similar to ours and the role of Sb in selective oxidation catalysts.

In general, activity for a dehydration reactions is related to the presence of acidic sites. Tanabe and co-workers (*2–5*) attempted to correlate general catalytic activity with the acidity and basicity of binary oxides. Ai *et al.* (*6–12*) measured the acidity and basicity of a great number of catalysts containing MoO_3. They found that the addition of another oxide to MoO_3 increased the acidity of the catalysts and concluded that the catalytic activity could be relatively well interpreted by the acid–base properties of catalysts. Belokopytov *et al.* (*13*) and Groff (*14*) detected Lewis and Brønsted sites on the surface of MoO_3. Tatibouët *et al.* (*15, 16*) postulated that the apical planes (001) + (101) and side plane (100) of the MoO_3 crystallites possessed the dehydrating sites. In a more recent study, Brückman *et al.* (*17*) concluded that the Brønsted acid sites were located on the (110), (001), and (101) faces of MoO_3 crystallites.

[1] Present address: Dalian Institute of Chemical Physics, Chinese Academy of Sciences, Dalian, China.

[2] On leave from the Institute of Catalysis and Surface Chemistry, Polish Academy of Sciences, Cracow, Poland.

0021-9517/91 $3.00

On the other hand, numerous studies have been devoted to catalysts containing antimony oxide, such as $FeSbO_4 + Sb_2O_4$, $SnO_2 + Sb_2O_4$, and $UO_3 + Sb_2O_4$. These studies are far from having clarified the role of antimony oxide. Boreskov and co-workers (*18, 19*) suggested that the excess antimony avoids the formation of free Fe_2O_3 which could be responsible for the total oxidation. Fattore *et al.* (*20*) confirmed that $FeSbO_4$ and Sb_2O_4, as separate phases, cooperate in producing acrolein from propene, giving a higher selectivity than each phase alone. They postulated that allylic radical formation takes place on Sb_2O_4 and that oxygen ions migrate from $FeSbO_4$ to Sb_2O_4. Aso *et al.* (*21*) postulated that the excess Sb_2O_4 brings about the formation of a particular specific surface structure which results in the production of surface oxygen species suitable for the selective oxidation. After further studies (*22*), they concluded that surface Sb ions provided adsorption sites for oxygen. A surface layer enriched in Sb would preferentially accomodate the type of surface oxygen which oxidizes olefins selectively. Burriesci *et al.* (*23*) suggested that the role of excess bulk antimony is to promote the formation of structurally distorted and defective $FeSbO_4$, in order to form oxygen vacancies. Such vacancies are possibly associated with adsorption sites for the oxygen species that is responsible for allylic oxidation. Teller *et al.* (*24*) hypothesized that α-Sb_2O_4 crystallites are oriented to the surface of $FeSbO_4$ where they create catalytically active sites not found in isolated phases. Centi and co-workers (*25, 26*) postulated that the formation of surface groups such as O=Sb=O could explain the observed increase of selectivity in selective oxidation. Volta *et al.* (*27*) noted that particular Sb–Sb arrangements on the surface, such as those at the (001) crystallographic plane of α-Sb_2O_4, are responsible for the high selectivity. More recently, Straguzzi *et al.* (*28*) suggested that one role of the antimony component is to ensure that the oxidation is selective by replacing the "active" oxygens, responsible for total oxidation, with the "inactive" oxygens found on the surface of antimony oxides, the other role being to allow the reoxidation of the catalysts.

The first objective of this work is to try to identify the active sites on MoO_3 and to analyse the role of α-Sb_2O_4 in the catalytic cooperation observed in N-ethyl formamide dehydration and in particular the role of spillover oxygen in the formation of active sites.

To detect the nature of active sites in the surface of oxides, chemisorption is often used and small molecules such as NH_3, pyridine and CO_2, serve as a probe. The information concerning this adsorption is usually deduced from infrared spectroscopy measurements (*29, 30*). Due to the very low surface area (2 m^2g^{-1}) and low transparency of our samples, the concentration of adsorbed species is too close to or below the detectability limit by the infrared techniques (*31*) and the method is very difficult to apply. Another classic method used for the detection of active sites is temperature-programmed desorption (TPD) of the adsorbed species. We used this method to measure the basicity (TPD of CO_2) and acidity (TPD of NH_3) of our samples.

In the preceding paper of this series (*1*) we showed that the decrease of propionitrile selectivity was associated with a loss of oxygen from the surface of molybdenum oxide. The degree of reduction decreased with the increase in α-Sb_2O_4 antimony in the sample. Carbon deposition on the surface of MoO_3 was also responsible for the decrease of activity. The presence of α-Sb_2O_4 in the mixtures decreased the quantity of carbon deposited on MoO_3. It was concluded that α-Sb_2O_4 acted as a regenerating phase. We gave arguments supporting the view that the role of α-Sb_2O_4 was to generate spillover oxygen. The second objective of this paper, therefore, is to elucidate how this oxygen spillover can regenerate deactivated sites (or maintain their activity) on MoO_3. In order to obtain experimental information con-

cerning these aspects, the following experiments were carried out. Previously reduced or carbon-contaminated molybdenum oxide was mixed with α-Sb_2O_4 and the mixtures were investigated in different reoxidation conditions using three techniques: thermoreoxidation to measure the degree of reoxidation; electron spin resonance (ESR) to detect the disappearance of Mo^{+5}; and carbon analysis to quantify the removal of coke on the samples.

In the final part of this paper we attempt to give an explanation as to why the structural properties of α-Sb_2O_4 could explain the efficiency of this phase in producing spillover oxygen, and we show that spillover oxygen brings about the formation of acid sites on MoO_3.

As the catalysts used in oxygen-aided N-ethyl formamide dehydration are similar to those active and selective in allylic oxidation, we conclude with a short comparison with selective oxidation.

2. EXPERIMENTAL METHODS

2.1. Sample Preparation

(*a*) *Pure oxides, Ms and MoiSb samples.* The preparation of the pure α-Sb_2O_4 (2 m^2g^{-1}), pure MoO_3 (2 m^2g^{-1}), mechanical mixtures of these oxides, Ms and impregnation of Mo ions on Sb_2O_4 support, MoiSb samples, was described in detail in the preceding paper of this series (*1*).

(*b*) *MoO_{3-x} and MoO_{3-y}.* Portions of our pure MoO_3 (3 g) were reduced in H_2 (60 ml/min) at 380°C for 10 h or at 150°C for 25 h; these were designated as MoO_{3-x} and MoO_{3-y}, respectively. Their BET surface areas were 7.6 and 2.5 m^2g^{-1}. The X-ray diffraction pattern of MoO_3 showed the presence of MoO_3 and MoO_2 in MoO_{3-x}. That of MoO_{3-y} was identical to unreduced MoO_3.

(*c*) *MoO_3C.* A MoO_3 sample, used as a catalyst in N-ethyl formamide dehydration in the absence of oxygen during 70 h, constituted the MoO_3 contaminated by carbon used in our experiments. It was designated as MoO_3C. Its BET surface area was 4.2 m^2g^{-1}.

These previously reduced or carbon-contaminated molybdenum oxides were mechanically mixed with α-Sb_2O_4 (suspension in *n*-pentane, stirring and evaporation (*1*)).

Powder mixtures of differing mass ratios, i.e.,

$$r = \frac{W_{MoO_3}}{W_{MoO_3} + W_{\alpha\text{-}Sb_2O_4}},$$

varying from $r = 0.0$ to $r = 1.0$ were prepared. The pure α-Sb_2O_4 ($r = 0.0$) and the pure MoO_3 ($r = 1.0$) were treated under the same conditions as the mixtures.

2.2. Basicity and Acidity Measurements

The temperature-programmed desorption (TPD) of CO_2 and NH_3 was used to detect the surface basicity and acidity respectively. TPD measurements were carried out using a versatile apparatus equipped with a thermal conductivity detector (*32*).

2.2.1. TPD of CO_2. About 0.2 g of sample were pretreated under helium at 450°C for 1 h, exposed to CO_2 at 25°C during 30 min, and flushed at that temperature with helium during 30 min. TPD measurements were carried out with a heating rate of 10°C min^{-1}, from 25 up to 450°C under a flow of helium.

2.2.2. TPD of NH_3. Two series of measurements were made. In the first series, a sample of ca. 0.2 g was pretreated under helium at 450°C for 1 h, exposed to NH_3 at 25°C during 30 min, and flushed at that temperature with helium during 30 min. TPD measurements were carried out from that temperature up to 450°C under a flow of helium, at a heating rate of 10°C/min^{-1}. The amounts of ammonia which desorbed (in μmol NH_3 g^{-1}) during these TPD runs were assumed to correspond to the total surface acidity of the samples studied.

In the second series of measurements, ca. 0.2 g of a standard mixture of composition $r = 0.5$ was reduced with H_2 at 150°C during 1 h, flushed with helium at 25°C, and exposed to NH_3 as before. The TPD run was

carried out from 25 up to 360°C. The sample was then reoxidized with O_2 (10% of O_2 in He) at 150°C during 1 h and the whole procedure was repeated.

The quantity of ammonia adsorbed by the samples was estimated by a calibration method, namely by comparing it with the integral thermal conductivity signals obtained with precisely known amounts of NH_3.

2.3. Reoxidation

The measurement of the degree of reoxidation and reduction of a previously reduced molybdenum oxide in the presence of α-Sb_2O_4 was carried out as follows.

2.3.1. Thermoreoxidation. In order to overcome the low sensibility of the thermoreoxidation technique, our MoO_{3-x} sample, a relatively deeply reduced molybdenum oxide, was used in the measurements.

Thermoreoxidation of α-Sb_2O_4 + MoO_{3-x} mixtures was carried out with a Setaram MTB 10-8 microbalance connected to a vacuum and a gas-handling system. The weight changes were recorded continuously. About 0.08 g of sample were used in each run. The sample was heated from 25 to 370°C (10°C/min) in a flow of 60 ml/min of helium (Air Liquide Belge, 99.995%). After 1 h at 370°C, helium was replaced with a flow of 60 ml/min of dried air (Air Liquide Belge, 99.999%). The isothermal reoxidation experiments were always carried out at 370°C.

Results are expressed as a percentage of MoO_{3-x} weight increase, i.e. $(\Delta m/m_{MoO_{3-x}})\%$ with $\Delta m = m_t - m_0$ and ${}^{m}MoO_{3-x} = m_0 r$, where m_t is the weight after t minutes, m_0 is the initial weight, and r is the mass ratio of MoO_3 weight to total weight of the sample.

2.3.2. Electron Spin Resonance (ESR). ESR gives the possibility of determining the degree of reduction of our samples by the measurement of the Mo^{+5} ions concentration. Thanks to the high sensitivity of ESR, a slight superficial reduction of MoO_3 is enough to give the Mo^{+5} signal. This technique allows us to investigate the surface oxidation state of MoO_3 without changing its structure. Our MoO_{3-y} sample, a slightly reduced molybdenum oxide, was chosen for this investigation.

The measurements were performed in an X-band Varian E-12 Spectrometer with double cavity. The modulation frequency was 100 kHz. The power of the incident microwave beam was 20 mW. The special device of the sample holder used for pretreatment and ESR measurements was described in Ref. (*33*).

About 0.30 g of sample (MoO_{3-y}) was outgased at 25°C for 1 h and heated with a rate of 10°C/min from 25°C to 130°C. Oxygen (Air Liquide Belge, 1% of O_2 99.995% + 99% of He 99.995%) was introduced and the reoxidation was carried out isothermally at 130°C. The spectra were recorded at different times.

In order to compare quantitatively the ESR spectra, the Mo^{+5} signal intensities were normalized with the equation

$$[Mo^{+5}]_{rel} = \frac{I\,\Delta H^2}{I_O} \cdot \frac{S_S}{S} \cdot \frac{1}{m} \cdot \frac{1}{r}, \qquad (1)$$

where I is the intensity of the signal characteristic of Mo^{5+}, ΔH is the width of the signal for Mo^{5+}, I_O is the intensity of the internal standard (pitch), S is the selected sensitivity of the apparatus during measurement, $S_S = 1.25.10^4$ is the standard sensitivity, m is the mass of the sample (g), and r is the mass ratio.

The relative intensity of Mo^{5+} ($[Mo^{5+}]_{rel}$) after normalization is divided by the amount of MoO_{3-y} present in the samples.

2.4. Analysis of Carbon Deposit

The α-Sb_2O_4 + MoO_3C mixtures were pretreated at 370°C in air for 10, 20, 40, and 80 min. An analysis of the carbon deposit still remaining on the samples was performed using the method proposed by Jones *et al.* (*34*). The sample was fired in O_2 (Air Liquide Belge, 99.995%) at 1200°C. The CO_2 produced was absorbed by a N,N-dimethylformamide solution and subsequently titrated by a 0.02 *M* tetra-*n*-butylammonium hydroxide solution.

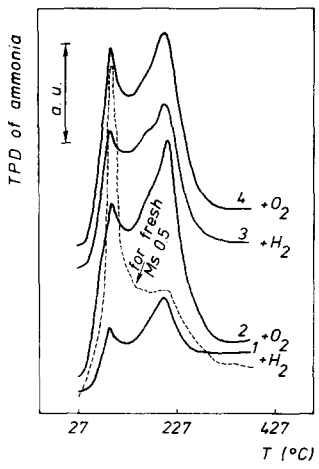

FIG. 1. NH_3 TPD profiles for the Ms 0.5 sample after different treatments: (1) reduction with H_2, (2) reoxidation with O_2, (3) second reduction with H_2, (4) second reoxidation with O_2. Dashed curve is the profile from the fresh Ms 0.5 sample.

The results are expressed using the formula

$$C\% = (W_c/W_{MoO_3C})\%$$

where W_c is the weight of carbon determined by the analysis and W_{MoO_3C} is the weight of MoO_3C in the analysed sample.

3. RESULTS

3.1. Basicity and Acidity

3.1.1. TPD of CO_2. CO_2 temperature-programmed desorption was carried out for the Ms0.0, Ms0.5 and Ms1.0 samples. No CO_2 desorption peak was observed.

3.1.2. TPD of NH_3. The TPD profile for Ms0.5 samples in the first series of measurements mentioned in Section 2.2.2. is presented in Fig. 1 (dashed line). Two overlapping peaks of NH_3 desorption with maxima at 110 and about 220°C are observed. The peak at 110°C is more intense than that at 220°C.

The amounts of NH_3 adsorbed by the Ms samples as a function of sample composition are presented in Fig. 2. Ms0.0 (namely pure α-Sb_2O_4) does not adsorb NH_3 at 25°C. The number of acidic centers increases with the concentration of MoO_3 in the sample until $r = 0.5$. The catalyst containing approximately equal quantities of α-Sb_2O_4 and MoO_3 possesses the maximum NH_3 adsorption capacity. Upon further increase of the MoO_3 content in the sample ($r > 0.5$) the amount of adsorbed NH_3 diminishes.

Figure 3 presents the TPD profiles of the MoiSb samples (impregnated samples). Two peaks of NH_3 desorption are also present, with maxima at 110 and 230°C. Contrary to the Ms samples, the peak at 110°C is less intense than that at 230°C. The former remains practically unchanged for the different samples while the latter increases with the MoO_3 content in the samples.

Table 1 gives the amounts of NH_3 adsorbed by the MoiSb samples. No NH_3 adsorption is detected for MoiSb0.0. After α-Sb_2O_4 is impregnated with a small amount of MoO_3, a conspicuous increase of NH_3 adsorption is observed. This adsorption increases with the content of MoO_3 in the samples.

Figure 1 presents the ammonia TPD profiles of the Ms0.5 sample obtained in the second series of measurements described in Section 2.2.2.

A mild reduction with hydrogen at 150°C decreases surface acidity (initially equivalent to 146 μm of NH_3 g^{-1}) by a factor of 3. The catalyst, when reoxidized with oxygen (10% of O_2 in He) at 150°C, recovers a high acidity, which diminishes again after the next reduction. After a new reoxidation, the

TABLE 1

Amount of NH_3 Adsorbed by MoiSb Samples

Samples	NH_3 adsorbed by sample (μmol/g cata.)	
	Before reaction	After reaction
MoiSb0.0%	0	
MoiSb0.075%	22	
MoiSb0.15%	33	30
MoiSb0.60%	39	40

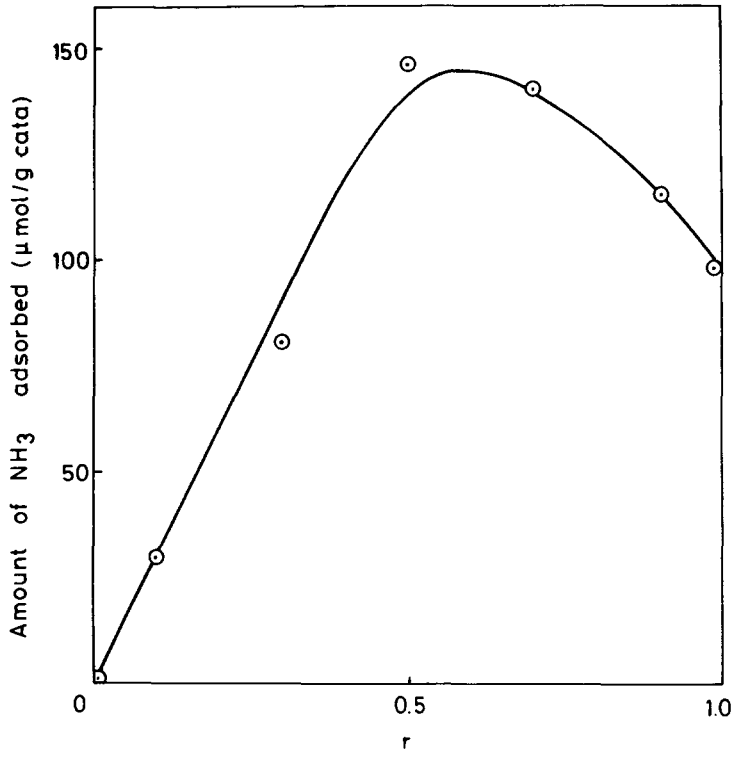

FIG. 2. Amount of NH_3 adsorbed by Ms as a function of the sample composition.

catalyst again regains a part of its initial acidity. The changes observed are mainly due to the peak at 220°C.

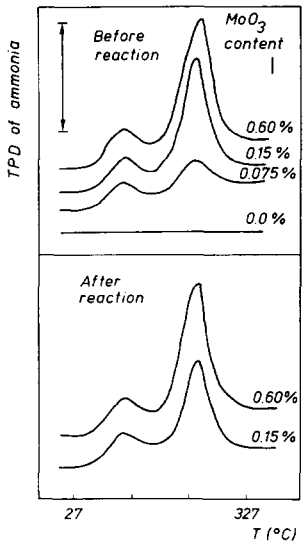

FIG. 3. NH_3 TPD profiles for MoiSb samples.

3.2. *Reoxidation of Previously Reduced Molybdenum Oxides*

3.2.1. Thermoreoxidation. Figure 4 presents the evolution of weight gain per amount of MoO_{3-x} contained in the samples with time during isothermal reoxidation at 370°C. At the beginning, some induction period is observed. The induction time for MoO_{3-x} ($r = 1.0$) is the longest. With the increase of α-Sb_2O_4 content in the samples, the induction time decreases progressively to zero. At any given time, the weight gain of MoO_{3-x} in the mixtures is greater than that of MoO_{3-x} alone. It increases with the α-Sb_2O_4 content in the samples.

The slope of the curves in Fig. 4, at the point at the inflexion point (end of induction time), is taken as an empirical rate. (This corresponds to the maximal rate of reoxidation). It is visible in Fig. 4 that the reoxidation reaction accelerates with the increase of α-Sb_2O_4 content in the samples.

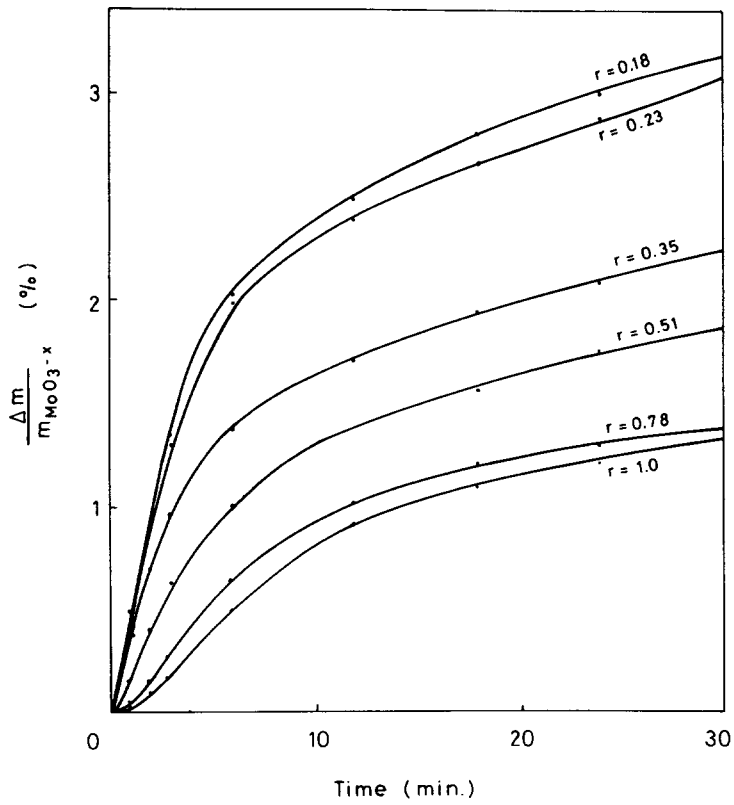

FIG. 4. Weight increase of MoO_{3-x} in α-Sb_2O_4 + MoO_{3-x} samples as a function of reoxidation time.

3.2.2. ESR measurements. ESR measurements were used to monitor the disappearance of Mo^{5+} during reoxidation. The samples containing MoO_{3-y} were chosen for this investigation. The relative intensities of the Mo^{5+} signal (g = 1.93; width: ca. 100 Gauss) as a function of reoxidation time are presented in Fig. 5. For all the samples, the Mo^{5+} intensities decrease with the reoxidation time. In MoO_{3-y} alone, the decrease of Mo^{5+} ions as a function of reoxidation time is almost linear. A marked curvature is observed for samples r = 0.7, 0.5, and 0.3; the aspect of the curves is practically the same for all three.

Before reoxidation (time 0), all samples contain practically the same quantity of Mo^{5+} ions. As soon as the reoxidation begins, the concentration of Mo^{5+} ions in the various mixtures always becomes lower than that in MoO_{3-y} alone, and the decrease is more rapid. The increase of α-Sb_2O_4 content in the mixtures accelerates this reoxidation.

3.3. Analysis of Carbon Deposit

The results of the analysis of carbon deposit as a function of pretreatment time are given in Fig. 6. The quantity of carbon remaining on the samples decreases with the increase of the treatment time. This decrease in the mixtures is more rapid than that in MoO_3C alone. At any given time, one notices that an increase of the α-Sb_2O_4 content in the mixtures up to r = 0.3 brings about a decrease of the remaining carbon quantity. A further increase of the α-Sb_2O_4 content in the mixture (from r = 0.3 to r = 0.1) has little effect.

4. DISCUSSION

The preceding paper (*1*) has shown that MoO_3 possesses the active sites and the role of α-Sb_2O_4 was to influence its cata-

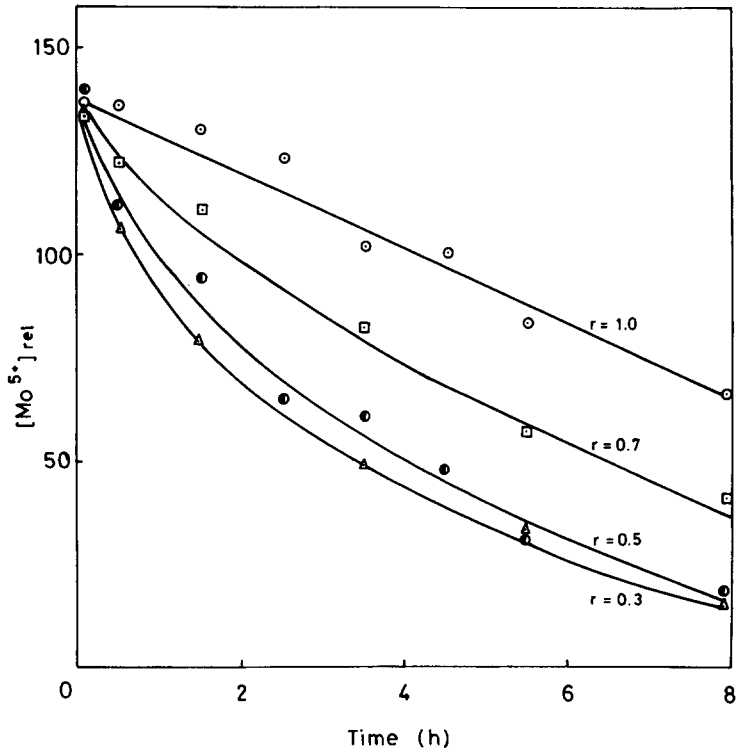

FIG. 5. $[M^{+5}]_{rel.}$ in α-Sb_2O_4 + MoO_{3-y} samples as a function of reoxidation time.

lytic activity in N-ethyl formamide dehydration. The discussion of the results of the present paper will focus on the following themes:

1. Basicity, acidity and nature of active sites;
2. Correlation between acidity and activity;
3. Influence of reduction and reoxidation on acidity;
4. Reoxidation of reduced molybdenum oxides;
5. Removal of carbon deposit;
6. Role of spillover oxygen and general correlation with catalytic activity;
7. Short comparison with selective oxidation.

4.1. Basicity, Acidity, and Nature of Active Sites

No CO_2 adsorption on the Ms samples was detected. Nevertheless, these results should not be taken as proof of a total absence of basic sites. Indeed, Ai (*7, 8, 9*) observed that pure MoO_3 did not adsorb CO_2 but adsorbed acetic acid. The author attributed this phenomenon to the difference in acid strength. Acetic acid is stronger than CO_2 and can adsorb on weak basic sites. With respect to our results, this means that our samples are devoid of relatively strong basic sites, but they might possess weak ones.

The NH_3 TPD results indicate the presence of two types NH_3 attached to the surface. They correspond to the desorption of NH_3 at 110°C, and in the 220–230°C temperature range, respectively.

These results should be compared with the findings of Belokopytov *et al.* (*13*) and Groff (*14*). The authors, in an infrared investigation of the acidity of MoO_3 by NH_3 adsorption, concluded that MoO_3 possesses (i) Lewis acid centers capable of adsorbing ammonia by the formation of a coordination

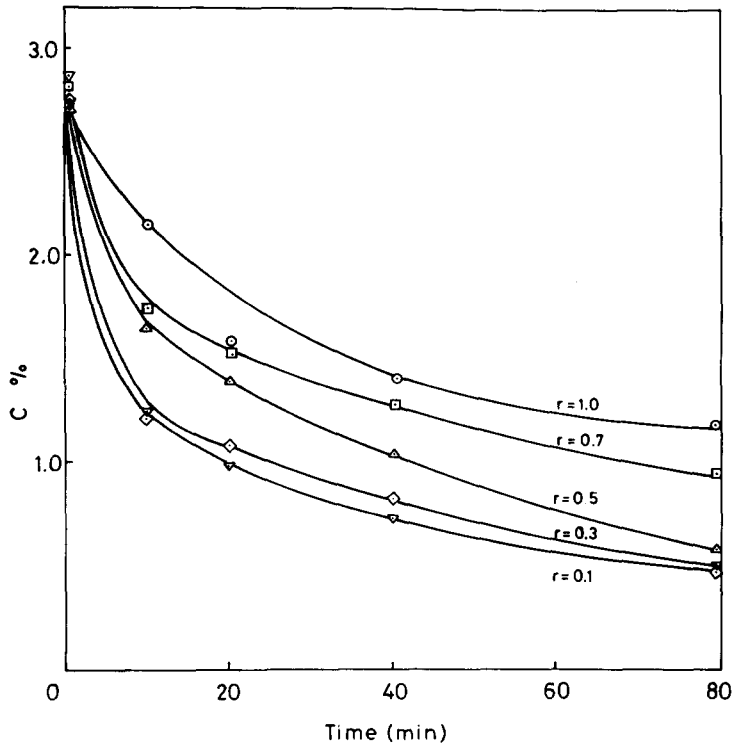

FIG. 6. Quantities of carbon deposit remaining on MoO_3 in α-Sb_2O_4 + MoO_3C samples as a function of pretreatment time.

bond and (ii) Brønsted centers, bringing about the formation of NH_4^+ ions. The bond between NH_3 and Lewis centers would be less strong than that with Brønsted centers (*13*). The IR band assigned to NH_3 adsorption on Brønsted sites disappeared only after evacuation at temperatures higher than 200°C. Taking into account these results, one can assign the second TPD peak (220–230°C) in Figs. 1 and 3 to NH_3 desorption from Brønsted sites.

The vast majority of mechanisms evoked to explain dehydration reactions involve Brønsted acid sites. Our previous results (*35*) led us to propose a concerted mechanism in which vicinal Brønsted acid (A) and basic (B) sites cooperated.

We do not exclude completely this mechanism. However, another mechanism can explain our results without having to evoke basic sites, the presence of which is not demonstrated in our work. This mechanism involves the intervention of a sole Brønsted acid site, and is presented in Scheme 1.

There is some difference of the NH_3 TPD profiles between Ms and MoiSb samples (Figs. 1 and 3): in the latter, the majority of the acid sites correspond to Brønsted ones whereas in the former, the two peaks are comparable in intensity. In the preceding paper (*1*), it has been shown that, in the Ms samples, MoO_3 formed large particles in the shape of plate-like crystallites exposing predominantly the (010) plane, whereas in the MoiSb samples, MoO_3 formed small particles with an important exposition of other planes, such as apical (001) + (101) and side ones (100). These morphologies could result in the differences in acid properties. In fact, the unsaturated oxygen ions on the (001), (101), and (100) planes (*36–38*) would be compensated for by a dissociative adsorption of water and this would produce Brønsted centers (*31*).

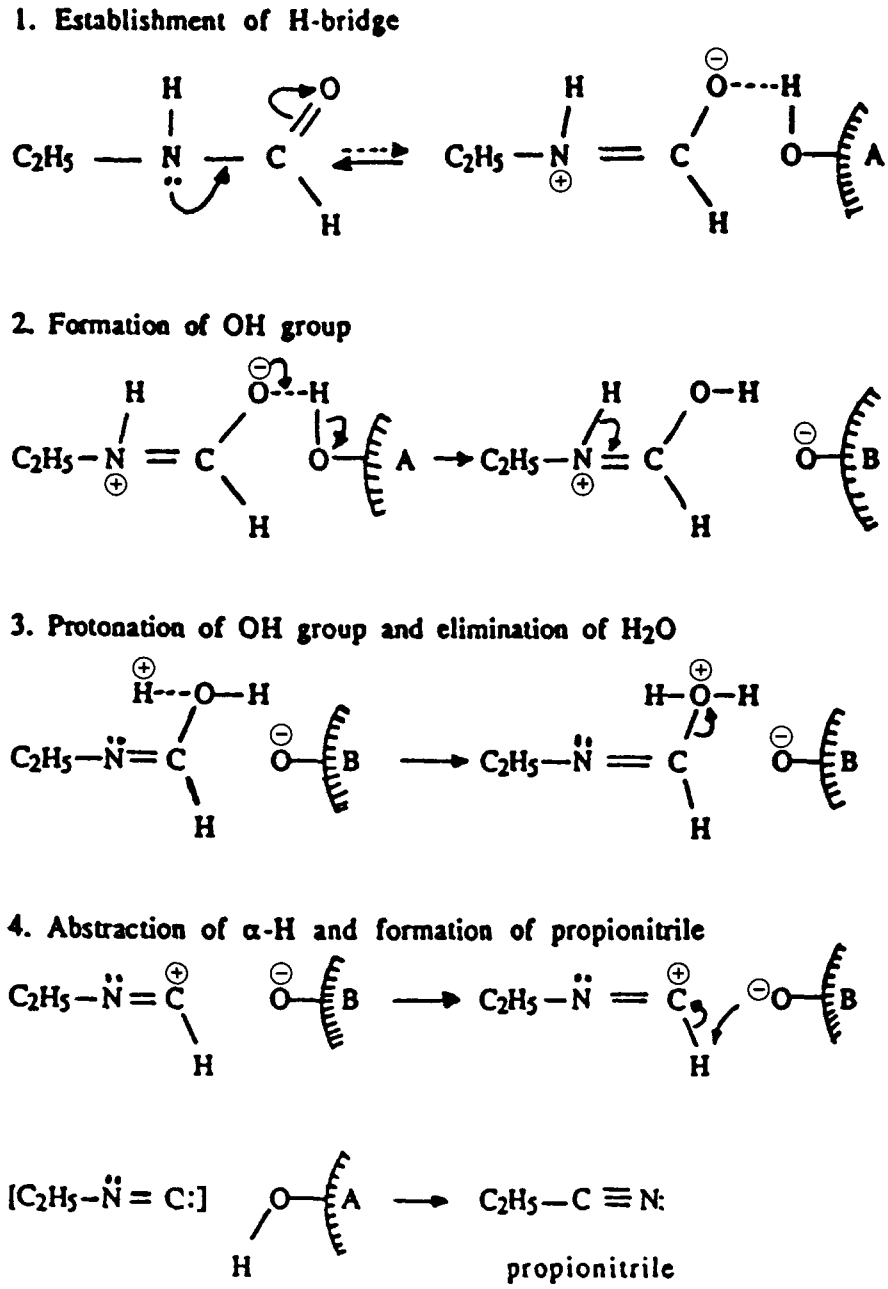

SCHEME 1. Mechanism of NEF dehydration involving Brønsted acid sites.

4.2. Correlation between Activity and Acidity

In the preceding paper (*1*), we observed that pure MoO_3 was active in N-ethyl formamide dehydration, contrary to α-Sb_2O_4. We concluded that the active sites are situated on MoO_3. When MoO_3 was in contact with α-Sb_2O_4, the activity increased conspicuously for both Ms and MoiSb samples.

The results in this paper indicate that α-Sb_2O_4 does not adsorb NH_3. On the con-

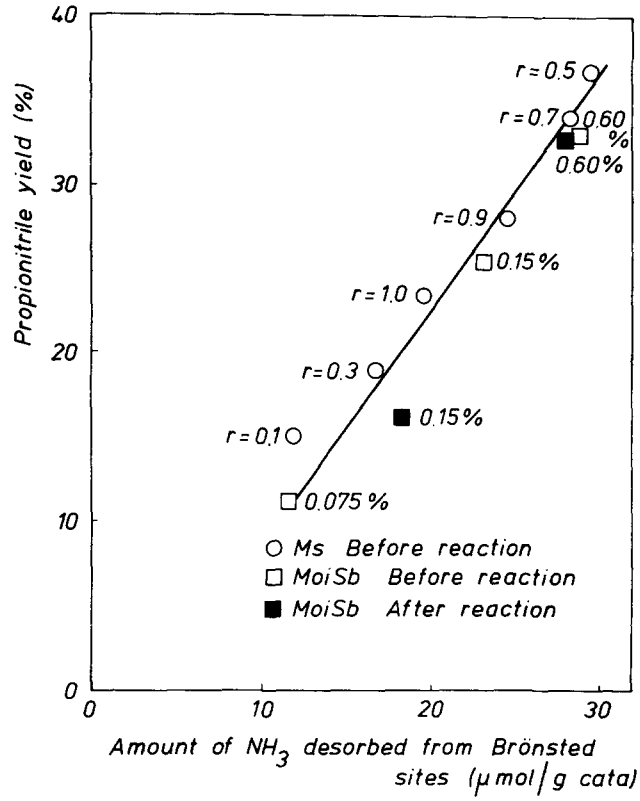

FIG. 7. Propionitrile yield as a function of amount of NH_3 desorbed from Brønsted sites of Ms and MoiSb samples.

trary, MoO_3 possesses the acid sites. The surface acidity increases remarkably when MoO_3 is in contact with α-Sb_2O_4 (Figs. 1, 2, and 3, and Table 1).

As the total amount of NH_3 desorbed from the MoiSb sample corresponds mainly to Brønsted sites, we could expect that a plot of dehydration activity vs. desorbed NH_3 would be approximately linear. This is indeed what we can observe. Account taken of the remark at the end of the preceding section, it is not surprising that we did not observe such a linearity with the Ms samples. For this reason, we separated the peaks corresponding to the two types of adsorption and took only the amount of NH_3 desorbed around 220°C (Brønsted sites). The corresponding plot of activity vs. NH_3 adsorbed is presented in Fig. 7. A good linear correlation between activity and Brønsted acidity is obtained. It is remarkable that the same correlation holds for both series of samples.

This proves that the activity is controlled by the number of Brønsted sites on the surface.

From these results, it is possible to calculate the turnover frequency on Brønsted sites. The propionitrile formed in the Ms 0.5 samples is 32.8 μmol min^{-1} m^{-2} and the amount of NH_3 desorbed from the Brønsted sites is 14.8 μmol m^{-2} (Fig. 7). The calculated turnover frequency is thus about 2 min^{-1}.

4.3. Influence of Reduction and Reoxidation on Acidity

In the first paper of this series (*1*), we have shown that the catalysts worked efficiently in N-ethyl formamide dehydration only in

the presence of gaseous oxygen. In this paper, we must try to explain how oxygen might modify the number of Brønsted sites.

As a whole, Fig. 1 shows an influence of the reducing–oxidizing treatment on both sites (Lewis and Brønsted). But reoxidation of reduced samples gives a conspicuous increase of TPD peaks corresponding to Brønsted sites (compare curves 1 and 3, corresponding to reduced samples, with curves 2 and 4, after reoxidation). This increase is more important than that corresponding to Lewis sites.

Generally, Brønsted sites cannot persist on the surface in the absence of water or precursors of hydroxyls. For explaining the results in Fig. 1, one can take into account the fact that MoO_3 can retain sufficient hydrogen in its shear structure (or as a MoO_3 "bronze") during the hydrogenation step (*39–41*), and that this hydrogen could form hydroxyls in the reoxidation step.

The TPD results of Fig. 1 thus gives proofs that oxygen can create or restore the useful Brønsted sites.

In the first series of measurements described in section 2.2.2, the Ms samples were pretreated in helium; no gaseous oxygen was present during the measurement. Nevertheless, the presence of α-Sb_2O_4 increased the surface acidity of the sample. In the following section, we show that the oxygens on the surface of α-Sb_2O_4 can migrate onto the surface of MoO_3; this can explain the creation or regeneration of the acid sites.

4.4. Reoxidation of Reduced Molybdenum Oxides

The reoxidation of the samples containing MoO_{3-x} shows that an increase of the α-Sb_2O_4 content in the mixture, decreases progressively the induction time to zero, and accelerates the rate of reoxidation.

When MoO_{3-x} is alone, the sole source of reoxidation is gaseous (molecular) oxygen O_2. When there is a contact with α-Sb_2O_4, another source is the mobile oxygen species activated by α-Sb_2O_4, which migrate onto the surface of MoO_{3-x}.

The acceleration of the reoxidation of MoO_{3-x} by α-Sb_2O_4 is an important proof of the migration of oxygen species from α-Sb_2O_4 onto MoO_{3-x}.

In general, reoxidation of reduced oxides is a process consisting of three steps:

1. adsorption of gaseous oxygen on the oxide surface;
2. dissociation of the adsorbed oxygen into a suitable oxygen species;
3. replenishment of this suitable oxygen species in the crystalline lattice.

The results presented in this paper strongly suggest that the rate determining step in the reoxydation of MoO_{3-x} would be the dissociation of oxygen; α-Sb_2O_4 could facilitate that dissociation.

The results and the conclusions are further confirmed by ESR measurements for the series of samples containing MoO_{3-y}. In that case, the MoO_3 sample is slightly reduced, and reduction is restricted to the superficial regions. The reoxidation is also accelerated by the presence of α-Sb_2O_4 in the samples.

4.5. Removal of Carbon Deposit

Under mild conditions, such as 370°C in air, carbon is removed only progressively. This permits us to measure the different quantities of carbon remaining on the samples after a series of treatment (Fig. 6). In principle, for a sample containing only MoO_3C, the carbon deposit can be removed either directly by molecular oxygen or by oxygen species coming from the surface of molybdenum oxide. When MoO_3C is in contact with α-Sb_2O_4, the removal of carbon is more rapid. An explanation consistent with those given above is that molecular oxygen is activated by α-Sb_2O_4 and is transferred to MoO_3C. If the particles of MoO_3C are surrounded by those of α-Sb_2O_4, many of the active oxygen species migrating from the surface of α-Sb_2O_4 could attack the carbon deposit. The decrease of the quantity of carbon deposit remaining on the samples when the α-Sb_2O_4 content in the samples increases (Fig. 6) indicates that this process plays an

important role in the reoxidation of deposited carbon.

4.6. *Role of Spillover Oxygen and General Correlation with Catalytic Activity*

The role of spillover oxygen has been discussed in the preceding paper (*1*). We concluded that it created the new active sites and/or regenerated the sites deactivated during the reaction. The deactivation was due to the reduction of MoO_3 and/or carbon deposition on MoO_3.

The results presented in this paper prove the validity of this interpretation. Indeed, the presence of α-Sb_2O_4 increases the surface acidity of Ms samples (Fig. 2); the reoxidation of the reduced molybdenum oxides, such as MoO_{3-x} or MoO_{3-y}, is facilitated by the presence of α-Sb_2O_4 in the samples (Figs. 4 and 5); and the surface of MoO_3 with a carbon deposit is more rapidly cleaned when in contact with α-Sb_2O_4 (Fig. 6). These results, even if alone, would strongly suggest that α-Sb_2O_4 can activate gaseous oxygen into a mobile species. They would also constitute proof of the existence of spillover oxygen. The formation and migration of spillover oxygen from α-Sb_2O_4 to MoO_3 has been proven by an independent experiment using ^{18}O (*42*). Taking all the results together, we are forced to come to the conclusion that spillover oxygen is involved in the creation of new active sites and regeneration of deactivated sites.

It is necessary to emphasize that no gaseous oxygen was present during the NH_3 TPD measurement of the first series (described in Section 2.2.2.). It is the oxygen on the surface of α-Sb_2O_4 that migrates onto the surface of MoO_3 where it creates the new acid sites. This creation is probably due to the fact, as shown in Fig. 8, that the oxygen ion migrating from α-Sb_2O_4 has a tendency to share its electrons with surface Mo^{6+} ions. This partially compensates the polarizing effects of the lattice oxygen atoms surrounding Mo, which tend to render Mo positive. This effect would result in increasing the density in negative charges of the unsaturated oxygen ions on, or above,

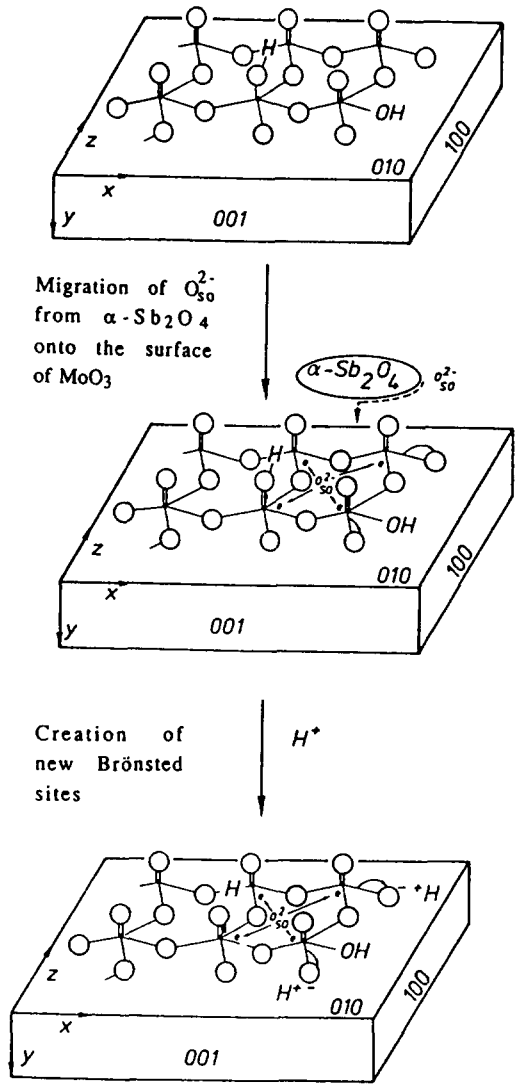

FIG. 8. Creation of new Brønsted sites by spillover oxygen: (•) molybdenum atom, (○) oxygen atom, (O^{2-}_{so}) spillover oxygen.

the surface, thus increasing the possibility of adsorbing a proton. The results would be the formation of Brønsted sites.

On the other hand, it should be noted that molybdenum oxides previously reduced or covered by carbon deposit were prepared in extremely severe conditions. Even in this case, the reoxidation and the removal of deposited carbon in conditions similar to those of N-ethyl formamide dehydration, i.e., 370°C in the presence of oxygen, take

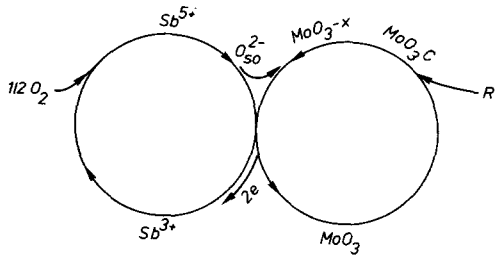

FIG. 9. Cycle of reoxydation and removal of carbon deposit by spillover oxygen.

place remarkably easily, especially for the sample containing α-Sb_2O_4. During "normal" N-ethyl formamide dehydration in the presence of oxygen, the reduction of part of the MoO_3 surface or coke formation certainly takes place only accidentally. It suffices that relatively few spillover oxygen species, activated by α-Sb_2O_4, could migrate onto the surface of MoO_3 for reoxidizing the reduced sites and cleaning the surface from coke.

We have thus a self-consistent explanation of the role of α-Sb_2O_4. By supplying spillover oxygen, it creates active sites and cleans the surface from coke deposit. It remains to discuss the reason of the efficiency of α-Sb_2O_4 in producing spillover oxygen.

The α-Sb_2O_4 is constituted by Sb^{5+} ions, which are in a distorted octahedral coordination with six strongly bonded oxygens, and Sb^{3+} ions, which are in a distorted pseudotrigonal–bipyramidal coordination with four strongly bonded oxygens and one weakly bonded oxygen (*43–45*). The characteristic of this structure gives the possibility to activate the oxygen, probably by a dissociation of one molecular oxygen into two oxygen ions. The adsorption of molecular oxygen can take place at the oxygen vacancy near Sb^{3+}. After the polarization and dissociation, the molecular oxygen becomes two O^{2-} ions, and the Sb^{3+} is oxidized to Sb^{5+}.

In a general way, the action of the reoxidation and the removal of carbon deposit could be described by the following equations:

$$Sb^{3+} + \tfrac{1}{2}O_2 \rightarrow Sb^{5+} + O^{2-} \quad (1)$$

$$Sb^{5+} + 2e^- \rightarrow Sb^{3+} \quad (2)$$

$$MoO_{3-x} + xO^{2-} \rightarrow MoO_3 + 2xe^- \quad (3)$$

$$MoO_3C + 2O^{2-} \rightarrow MoO_3 + CO_2 + 4e^-. \quad (4)$$

The electrons released by the reactions (3) and (4) could be accepted by Sb^{5+} at the contact region of α-Sb_2O_4 with MoO_3. After capture of electrons, Sb^{5+} becomes Sb^{3+} (reaction (2)). This provokes other oxygen vacancy for the dissociative adsorption of molecular oxygen.

This whole process, as shown in Fig. 9, constitutes a cycle which could operate many times during the catalytic reaction.

4.7. Short Comparison with Selective Oxidation

When our results are compared with those in literature concerning the role of α-Sb_2O_4 in other catalytic systems, especially in the $FeSbO_4$ + Sb_2O_4 catalysts, some parallelism could be expected. Straguzzi *et al.* (*28*) noted that although the involvement of Sb ions in the reaction cannot be ruled out, the primary function of the antimony appears to be to adsorb oxygen from the gas phase and that the oxygen, after dissociative adsorption on the antimony, leads to the reoxidation of the catalyst. The cooperation of Sb^{5+} and Sb^{3+}, i.e., the capture of electrons by Sb^{5+} and the adsorption of molecular oxygen from the gas phase by vacancies near Sb^{3+}, are indeed a process of Sb^{5+} reduction and Sb^{3+} reoxidation during reaction. This phenomenon was observed by Kriegsmann *et al.* (*46*) and Straguzzi *et al.* (*47*).

Our results certainly agree with the literature in that they point to the critical role of antimony with respect to oxygen activation.

They shed light on the mechanism and in particular on site formation, which has a direct bearing on selective oxidation.

The fact that Sb_2O_4 acts via a remote con-

trol mechanism in formamide dehydration suggests that a remote control mechanism might also work in selective oxidation. In this way it contributes to the understanding of the role of antimony in a multicomponent catalyst.

The research concerning the desirable catalyst properties in selective oxidation reactions has received more and more attention in recent years (*48*). Although a consensus has not been reached, some trends can be discerned. One of the interesting approaches consists in explaining the role of acid–basic and redox properties in selective oxidation (*31, 48*).

The acido-basic properties may play a role in many steps of the selective oxidation. As postulated by Grzybowska (*31*), the adsorption and activation of hydrocarbons can be considered as an acido-basic process, olefins being adsorbed on exposed metal cations (Lewis centers) with abstraction of hydrogen on oxygen ions (Lewis bases). Such an approach implies direct correlation between activity and acidity for the reactions in which the activated adsorption is a rate-determining step. Acido-basic properties may also be involved in regulating the energetics and kinetics of the adsorption–desorption steps of the reaction products and thus may influence the selectivity of various products formed in the consecutive route of the oxidation. High acidity of a catalyst may bring about a strong adsorption of reactants, which may then react further on the surface without desorption to the gas phase, giving undesirable CO_2. Ai *et al.* (*6–12*) suggested, that the oxidation reaction of the base–base type (e.g., butene to butadiene) requires the presence of both acidic centers (for butene adsorption) and basic ones (to facilitate butadiene desorption), whereas for the base–acid reaction (butene to maleic anhydride) the acidic centers are necessary to facilitate both adsorption of substrate and desorption of a product.

The redox properties of the selective oxidation catalysts have been largely studied in the literature. It is well known that a good selective oxidation catalyst, after its lattice oxygen takes part in the reaction, should be capable of replenishing the formed vacancy with the oxygen species activated by an element in the catalyst (*49–56*).

The work presented here can provide valuable clues for establishing a correlation between activity and acido-basic as well as redox properties of catalyst.

5. CONCLUSIONS

The experiments presented in this paper were designed to identify the nature of active sites and to investigate the role of spillover oxygen.

Our results show clearly that the Brønsted sites situated on the surface of MoO_3 are necessary for the dehydration of N-ethyl formamide. For this reaction a mechanism involving only Brønsted sites can be considered. The number of these sites and, in a similar manner, the catalytic activity can be influenced by the presence of α-Sb_2O_4 in the catalysts.

Reduction of MoO_3 has been considered as one of the reasons for deactivation. Reoxidation of previously reduced molybdenum oxides indicates that the rate-determining step is the dissociation of molecular oxygen into a suitable oxygen species which can replenish the crystalline lattice. The α-Sb_2O_4 facilitates that dissociation. The supply of dissociated oxygen species by migration from α-Sb_2O_4 onto the surface of MoO_3 permits or accelerates the reoxidation. Reoxidation is accompanied by reformation of the Brønsted sites.

Carbon deposition on the surface of MoO_3 is another reason for deactivation probably narrowly linked with the first. Oxidation of carbon deposits on the surface of MoO_3 demonstrates that the oxygen species, activated by α-Sb_2O_4, can remove the carbon deposits more efficiently than gaseous oxygen.

In conclusion, α-Sb_2O_4 can produce spillover oxygen by dissociation of molecular oxygen into oxygen ions. These oxygens

can migrate from α-Sb_2O_4 onto the surface of MoO_3 where they create the new Brønsted sites and/or regenerate the sites deactivated by reduction of catalysts and deposition of carbon.

ACKNOWLEDGMENTS

We are very much indebted to Professor K. Tanabe for the fruitful discussions we had during a stay he made in our laboratory, and especially for the discussions on the mechanism of N-ethyl formamide dehydration.

The financial support of the Commissariat Général aux Relations Internationales de la Communauté Française de Belgique (B. Zhou) and the Service de Programmation de la Politique Scientifique (P. Ruiz, T. Machej) is gratefully acknowledged. We are indebted to M. Genet for the constructive discussions and comments.

The authors thank Professor P. Cloos, Dr. O. B. Nagy, and Dr. J. L. Dallons for their useful comments and suggestions.

REFERENCES

1. Zhou, B., Sham, E., Bertrand, P., Machej, T., Ruiz, P., and Delmon, B., *J. Catal.* **132**(1), 157 (1991).
2. Shibata, K., Kiyoura, T., Kitagawa, J., and Tanabe, K., *Bull. Chem. Soc. Jpn.* **46**, 2985 (1973).
3. Tanabe, K., Shibata, T., Kiyoura, and Kitagawa, J., *Bull. Chem. Soc. Jpn.* **47**, 1064 (1974).
4. Itoh, M., Hattori, H., and Tanabe, K., *J. Catal.* **35**, 225 (1974).
5. Jin, T., Hattori, H., and Tanabe, K., *Bull. Chem. Soc. Jpn.* **55**, 2279 (1982).
6. Ai, M., and Suzuki, S., *J. Catal.* **26**, 202 (1972).
7. Ai, M., and Suzuki, S., *J. Catal.* **30**, 362 (1973).
8. Ai, M., *J. Catal.* **40**, 327 (1975).
9. Ai, M., *Bull. Chem. Soc. Jpn.* **49**(5), 1328 (1976).
10. Ai, M., *J. Catal.* **50**, 291 (1977).
11. Ai, M., *J. Catal.* **52**, 16 (1978).
12. Ai, M., *Bull. Chem. Soc. Jpn.* **56**, 862 (1983).
13. Belokopytov, W., Yu, V., Kholyavenko, K. M., Gerei, S. V., *J. Catal.* **60**, 1 (1979).
14. Groff, R. P., *J. Catal.* **86**, 215 (1984).
15. Tatibouët, J. M., and Germain, J. E., *J. Catal.* **72**, 375 (1981).
16. Tatibouët, J. M., Germain, J. E., and Volta, J. C., *J. Catal.* **82**, 240 (1983).
17. Brückman, K., Grabowski, R., Haber, J., Mazurkiewicz, A., Slozynski, J., and Wiltowski, T., *J. Catal.* **104**, 71 (1987).
18. Boreskov, G. K., Vent' yaminov, S. A., Dzis'ko, V. A., Tarasova, D. V., Dindoin, V. M., Sazonova, M. M., Olen'kova, T. P., and Keiefi, L. M., *Kinet. Catal.* **10**, 1350 (1969).
19. Shchukin, V. P., Boreskov, G. K., Ven'yaminov, S. A., and Tarasova, D. V., *Kinet. Catal. Engl. Transl.* **11**, 153 (1970).
20. Fattore, V., Fuhrman, Z. A., Manara, G., and Notari, B., *J. Catal.* **37**, 223 (1975).
21. Aso, I., Furukawa, S., Yamazoe, N., and Seiyama, T., *J. Catal.* **64**, 29 (1980).
22. Yamazoe, N., Aso, I., Amamoto, T., and Seiyama, T., *in* "Proceedings, 7th International Congress on Catalysis, Tokyo, 1980," p. 1239. Elsevier, Amsterdam, 1981.
23. Burriesci, N., Garbassi, F., Petrera, M., and Petrini, G., *J. Chem. Soc. Faraday Trans. 1* **78**, 817 (1982).
24. Teller, R. G., Brazdil, J. F., Grasselli, R. K., *J. Chem. Soc. Faraday Trans. 1* **81**, 1693 (1985).
25. Centi, G., Trifiro, F., *Catal. Rev. Sci. Eng.* **28** (2 & 3), 165 (1986).
26. Carbucicchio, M., Centi, G., and Trifiro, F., *J. Catal.* **91**, 85 (1985).
27. Volta, J. C., Bussiere, P., Coudurier, G., Herrmann, J. M., and Vedrine, J. C., *Appl. Catal.* **16**, 315 (1985).
28. Straguzzi, G. I., Bischoff, K. B., Koch, T. A., and Schuit, G. C. A., *J. Catal.* **104**, 47 (1987).
29. Busca, G., and Lorenzelli, V., *Mater. Chem.* **7**, 89 (1982).
30. Kung, M. C., and Kung, H. H., *Catal. Rev. Sci. Eng.* **27**, 452 (1985).
31. Grzybowska-Swierkosz, B., *Mater. Chem. Phys.* **17**, 121 (1987).
32. André, O., "Thesis, Faculté des Sciences Agronomiques, Université Catholique de Louvain, 1985."
33. Tascon, J. M. D., Mestdagh, M. M., and Delmon, B., *J. Catal.* **97**, 312 (1986).
34. Jones, R. F., Gale, P., Hopkins, P., and Powell, L. N., *Analyst (London)* **90**, 623 (1965).
35. Ceckiewicz, S., and Delmon, B., *Bull. Soc. Chim. Belg.* **93**, 163 (1984).
36. Tatibouët, J. M., *C.R. Seances Acad. Sci. Ser. 2:* **297**(II), 703 (1983).
37. Ziolkowski, J., *J. Catal.* **80**, 263 (1983).
38. Volta, J. C., Forissier, M., Theobold, F., and Pham, T. P., *Chem. Commun. Faraday Discus* **72**, 225 (1981).
39. Dickens, P. G., Birtill, J. J., and Wright, C. J., *J. Solid State Chem.* **28**, 185 (1979).
40. Birtill, J. J., and Dickens, P. G., *J. Solid State Chem.* **28**, 367 (1979).
41. Slade, R. C. T., Halstead, J. K., and Dickens, P. G., *J. Solid State Chem.* **34**, 183 (1980).
42. Weng, L. T., Duprez, D., Ruiz, P., Delmon, B., *J. Mol. Catal.* **52**, 349 (1989).
43. Thornton, G., *Acta Crystallogr. Sect. B* **33**, 1271 (1977).
44. Gopalakrishnan, P. S., and Manohar, H., *Cryst. Struct. Commun.* **4**, 203 (1975).

45. Teller, R. G., Antonio, M. R., Brazdil, J. F., Grasselli, R. K., *J. Solid State Chem.* **64,** 249 (1986).
46. Kriegsmann, H., Ohlmann, G., Scheve, J., Ultrich, F. J., *in* "Proceedings, 6th International Congress on Catalysis, London, 1976," Vol. 2, p. 836. The Chemical Society, London, 1977.
47. Straguzzi, G. I., Bischoff, K. B., Koch, T. A., Schuit, G. C. A., *Appl. Catal.* **25,** 257 (1986).
48. Kung, H. H., *Ind. Eng. Chem. Prod. Res. Dev.* **25,** 171 (1986).
49. Keulks, G. W., *J. Catal.* **19,** 232 (1970).
50. Wragg, R. V., Ashmore, P. G., and Hockey, J. A., *J. Catal.* **22,** 49 (1971).
51. Haber, J., *in* "Proceedings, 8th International Congress on Catalysis, Berlin, 1984," Vol. I, p. 85. Dechema, Frankfurt-am-Main, 1984.
52. Hucknall, D. J., "Selective Oxidation of Hydrocarbons." Academic Press, New York/London, 1974.
53. Schuit, C. C. A., *J. Less-Common Met.* **36,** 329 (1974).
54. Callahan, J. L., Grasselli, R. K., Milberger, E. C., and Strecher, H. A., *Ind. Eng. Chem. Proc. Res. Dev.* **9,** 134 (1970).
55. Brazdil, J. F., Suresh, D. D., and Grasselli, R. K., *J. Catal.* **66,** 387 (1980).
56. Dadyburjor, D. B., Jewur, S. S. and Ruckenstein, E., *Catal. Rev. Sci. Eng.* **19**(2), 293 (1979).